ICAS-92-2.5R

A NUMERICAL STUDY OF SLIT V-GUTTER FLOWS

Y. M. Tsuei
Chung-Shan Institute of Science and Technology

D. Lee
Institute of Aeronautics and Astronautics
National Cheng Kung University
Taiwan, China

ABSTRACT

In this study, both the non-reacting and the reacting flowfields of a slit V-gutter are investigated numerically. The flow pattern is found to be significantly different from that of a conventional V-gutter. For a small slit height h, two separate recirculation bubbles are formed. A smaller bubble is anchored behind the inner gutter, a larger one follows. With a larger h, the smaller bubble grows and the larger one shrinks. As h increases further, the two bubbles merge to form a single recirculation zone. The magnitude and the angle of the slit velocity play important roles in determining the strength of the recirculation zone. These results are consistent with the in-house, experimental observation. It is also found that an adequate gutter configuration can provide lower pattern factor and higher energy content in the recirculation zone as compared to a conventional gutter.

INTRODUCTION

Studies of turbojet engines have shown that substantial performance gains are possible by increasing the mass flow of air per unit of engine frontal area. However, the full advantage of this development cannot be exploited unless good combustion efficiency at high velocity levels can be achieved in both the main combustor and the afterburner. To stabilize a flame in a high velocity stream, a region whose velocity is lower than the burning velocity of the mixture should be created so that flames can be anchored and provide a continuous ignition source to the fresh mixture. A flameholder is devised to serve this purpose. Studies of use of flameholders in a high velocity afterburner are dated back to 1950's[1-4]. More detailed discussions can be found, among others, in Ref. [5,6]. Evidences show that the arrangement of flameholders is one of the dominant factors affecting afterburner performance. The best arrangement of flameholder is a function of the factors of environment in which the flameholder must operate. It is, therefore, obvious that a single optimum arrangement of flameholders does not exist for all possible environment conditions. With advances in numerical simulation techniques, various parametric studies can be conducted more cost-effectively to aid the design. The solver employed here is developed previously. A primary-variable formulation and a body-fitted coordinate system with non-staggered grid arrangement are used[7,8].

In this study, the flow fields of a slit V-gutter with half angle of 45 degree are simulated. The configuration of the slit V-gutter is shown in Fig. 1. This flameholder is reported to yield a more stable and reliable flame. An extinction limit at lower fuel/air ratio and a higher combustion efficiency are also reported[9]. To simplify the cases, the flow field upstream of the gutter will not be considered. The Reynolds number based on the main stream velocity is 45000. The effect of the slit height h, the slit flow velocity V_1 and its angle A on the flow field are studied. Two combustion models are employed, the fast chemistry model and the eddy-break-up model. The differences in predictions are addressed.

NUMERICAL ASPECTS

The governing equations and the turbulence model equations can be expressed

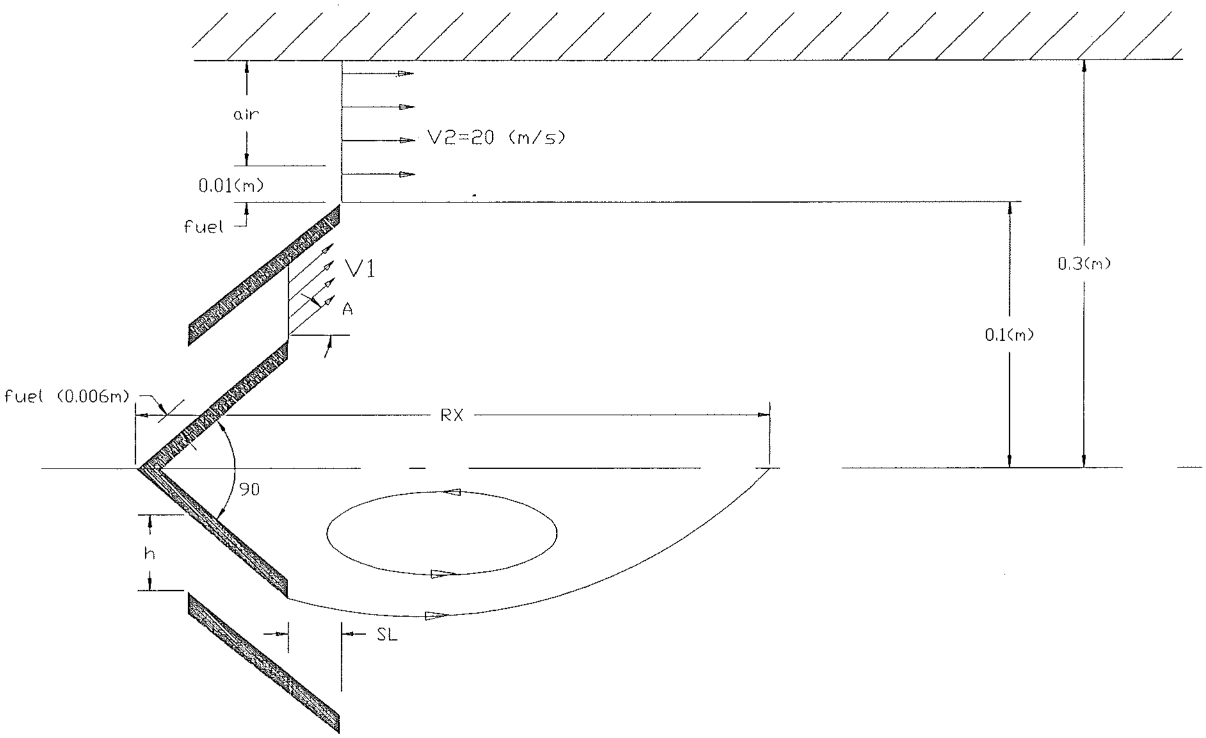

Fig. 1 The Configuration of a Slit V-gutter.

in the following unified form as

$$\frac{\partial}{\partial t}(\rho\Phi) + \mathrm{div}(\rho V\Phi) = \mathrm{div}(\Gamma^{\Phi}\mathrm{grad}\Phi) + R^{\Phi} \tag{1}$$

where Φ represents the dependent variable, Γ^{Φ} is the effective diffusion coefficient of variable Φ and R^{Φ} is the lumped source term for the equation. In order to treat the flow in complex geometries and to incorporate boundary conditions more conveniently and accurately. The above equation is transformed to a non-orthogonal body-fitted coordinate system, and this leads to

$$\frac{\partial}{\partial t}(\sqrt{g}\rho\Phi) + \frac{\partial}{\partial q^j}(\sqrt{g}\rho V^j\Phi) = \frac{\partial}{\partial q^j}\left(\sqrt{g}g^{jk}\Gamma^{\Phi}\frac{\partial\Phi}{\partial q^k}\right) + \sqrt{g}R^{\Phi} \tag{2}$$

where V^j is the contravariant velocity, g^{jk} is the metric tensor, q^j and q^k are the general coordinates and $\sqrt{g}$ is the Jacobian. For a two-dimensional, steady, incompressible flow, the governing equation becomes

$$\frac{\partial}{\partial\xi}(\sqrt{g}\rho U\Phi) + \frac{\partial}{\partial\eta}(\sqrt{g}\rho V\Phi) = \frac{\partial}{\partial\xi}\left(\sqrt{g}g^{11}\Gamma^{\Phi}\frac{\partial\Phi}{\partial\xi}\right) + \frac{\partial}{\partial\eta}\left(\sqrt{g}g^{22}\Gamma^{\Phi}\frac{\partial\Phi}{\partial\eta}\right) + S^{\Phi} \tag{3}$$

where

$$S^{\Phi} = \sqrt{g}\ R^{\Phi} + C^{\Phi}$$

$$C^{\Phi} = \frac{\partial}{\partial\xi}(\sqrt{g}\,g^{12}\Gamma^{\Phi}\frac{\partial\Phi}{\partial\eta}) + \frac{\partial}{\partial\eta}(\sqrt{g}\,g^{21}\Gamma^{\Phi}\frac{\partial\Phi}{\partial\xi})$$

$$\sqrt{g} = x_{\xi}y_{\eta} - x_{\eta}y_{\xi} \qquad g^{12} = g^{21} = -(x_{\xi}x_{\eta} + y_{\xi}y_{\eta})/g$$

$$g^{11} = (x_{\eta}^2 + y_{\eta}^2)/g \qquad g^{22} = (x_{\xi}^2 + y_{\xi}^2)/g$$

$$U = (uy_{\eta} - vx_{\eta})/\sqrt{g} \qquad V = (vx_{\xi} - uy_{\xi})/\sqrt{g}$$

Eqn. (3) can be discretized by using various differencing schemes and the final form of discretized equation at the grid point P becomes

$$A_P\Phi_P = \sum_{i=W,E,N,S} A_i\Phi_i + S_P \tag{4}$$

The discretized equation (4) along with a pressure correction equation, can be solved with the SIMPLE algorithm[10]. Nine equations are to be solved when eddy-break-up model is employed. These equations are the pressure correction equation, two momentum equations, k, ε equations, conserved scalar f equation, its variance g equation, fuel mass fraction Y_F equation and its variance g_{fu}.

In the present study, the grid cell structure for the various physical variables is a non-staggered system. Physical variables of a grid node are stored at the same location and sharing the same control volume[11]. This can simplify the cell structure particularly when application is extended to a three-dimensional problem.

In the eddy-viscosity approach for turbulence model, the most popular choice is the K-ε model which solves the transport equations for turbulence kinetic energy K and its dissipation rate ε. The transport equations for K and ε can be cast in the same form of Eq. (1). The diffusion coefficients and source terms are

$$\Gamma^k = \mu_{eff}/\sigma^k \quad \text{and} \quad R^k = G - \rho\varepsilon \qquad \text{for K equation}$$

$$\Gamma^\varepsilon = \mu_{eff}/\sigma^\varepsilon \quad \text{and} \quad R^\varepsilon = \frac{\varepsilon}{K}(C_1 G - C_2 \rho\varepsilon) \qquad \text{for } \varepsilon \text{ equation}$$

$$G = -\rho\overline{u_i u_j}\frac{\partial V_i}{\partial x_j} \tag{5}$$

where μ_{eff} is the effective viscosity and G is the generation rate of turbulence kinetic energy, and C_1, C_2 are constants.

In the eddy-break-up model, the source term for the fuel mass fraction Y_f equation is $-\bar{\omega}_{fu}$[12] where

$$\bar{\omega}_{fu} = \text{Min}\,[\,\bar{R}_{fu}, \bar{R}_{EBU}\,] \tag{6}$$

and

$$\bar{R}_{fu} = A\,\bar{\rho}^2\bar{Y}_f\bar{Y}_o \exp(-E/RT)$$

$$\bar{R}_{EBU} = C_r\bar{\rho}\frac{\varepsilon}{k}\sqrt{g_{fu}}$$

with Cr=4.0 as used in Ref. [13]. Namely, the source term is determined by the eddy-break-up rate or the reaction rate, whichever is the smaller. The source term of the variance g_{fu} equation is modelled as :

$$C_{g1}G_{fu} - C_{g2}\,\bar{\rho}\frac{\varepsilon}{k}g_{fu} - R_g \tag{7}$$

and

$$G_{fu} = \mu_{eff}\left(\frac{\partial\bar{Y}_f}{\partial x_j}\right)^2$$

where C_{g1} and C_{g2} are constants, μ_{eff} is the effective viscosity. R_g represents the kinetic rate term for the variance g_{fu} equation. In many cases, the convection and diffusion terms are small. If they are simply neglected, the above g_{fu} equation will be an algebraic one. Further simplification is also possible by dropping the reaction rate term in Eq. (6) as suggested in Ref. [13]. In the present study, we adopted this approach.

In this study, we define the following parameters:

1. reversed mass flow rate:

$$\dot{m} = \int \rho\,|u|\,dxdy \qquad \text{for } u \le 0$$

2. energy content in the reversed flow

$$\dot{H} = \int \rho\,C_p T\,|u|\,dxdy \quad \text{for } u \le 0$$

where Cp is the specific heat

3. pattern factor

$$p_f = \frac{T_{max} - T_4}{T_4 - T_3}$$

where T_{max} is the maximum temperature in the flow field, T_3 is the averaged inlet temperature and T_4 is the averaged outflow temperature. Smaller pattern factor implies a more uniform temperature distribution.

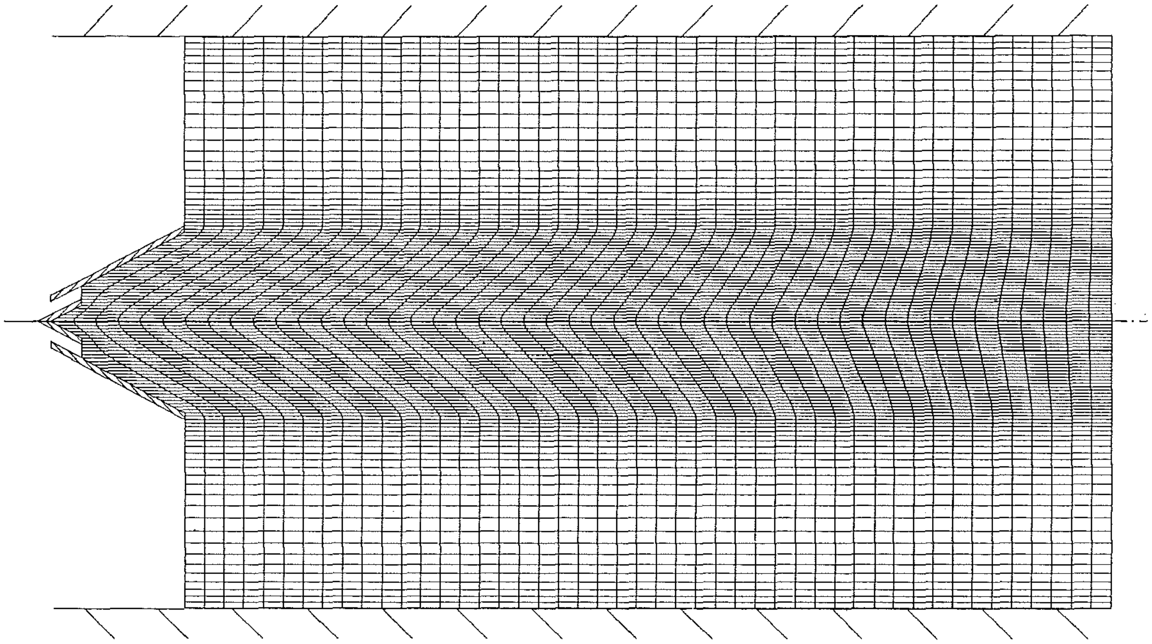

Fig. 2 The Grid for a Slit V-gutter.

NUMERICAL FLOW VISUALIZATION

The configuration and the dimensions of the slit V-gutter is shown in Fig.1. V_1 is the slit flow velocity, and A is its angle. V_2 is the main stream velocity. SL is the staggering distance between the trailing edges of the inner and the outer rings. RX represents the length of the recirculation bubble, and RY, its width. A two-dimensional grid generator LT-GRID developed by the authors has been used to create the initial grid[14]. The grid generator is based on solving the elliptic equations which govern the distribution of grids. The total grid used is 48x60. The resulting grid is demonstrated in Fig. 2. The Reynolds numbers based on the main stream velocity and the diameter of the pipe are 200 for the laminar cases and 45000 for the turbulent flows.

Our preliminary results show that the flow patterns of a slit V-gutter can be quite different from those of a conventional V-gutter[15]. The flow pattern changes successively as the slit height h increases. For a small h, two separate recirculation bubbles are formed. A smaller bubble anchors behind the inner gutter, a larger one follows. These two bubbles are induced by the slit flow and the main stream respectively. As h increases, the smaller

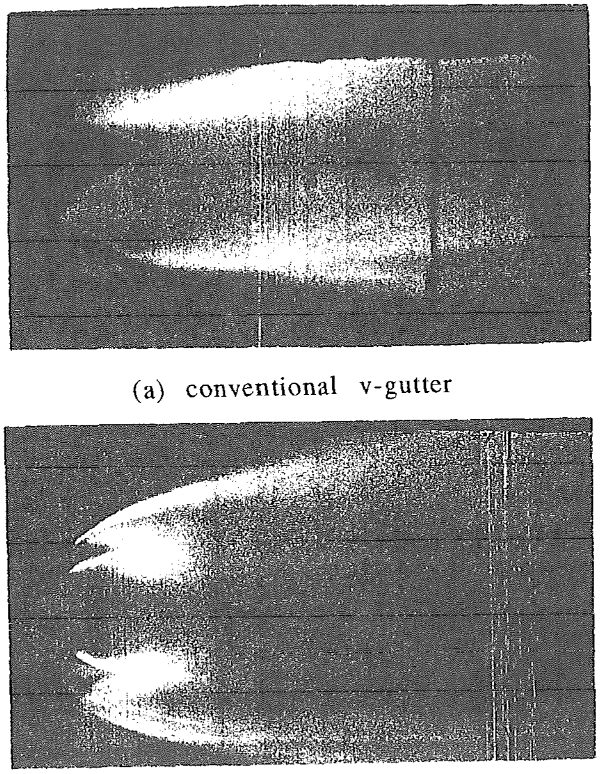

(a) conventional v-gutter

(b) slit v-gutter

Fig. 3 Experimental Visualization of the Reacting Flows (Provided by Prof. M. R. Wang, IAA)

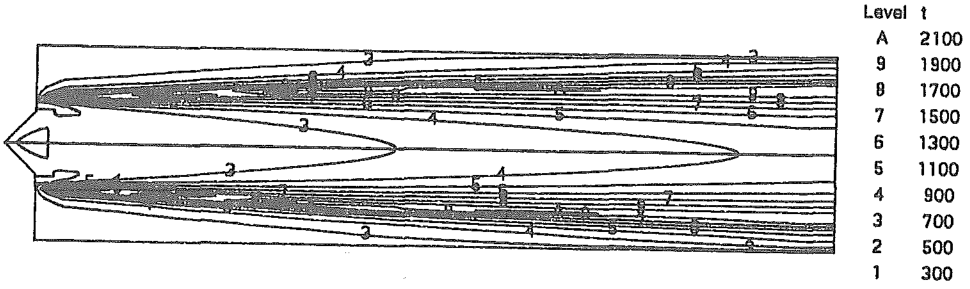

(a) a conventional v-gutter

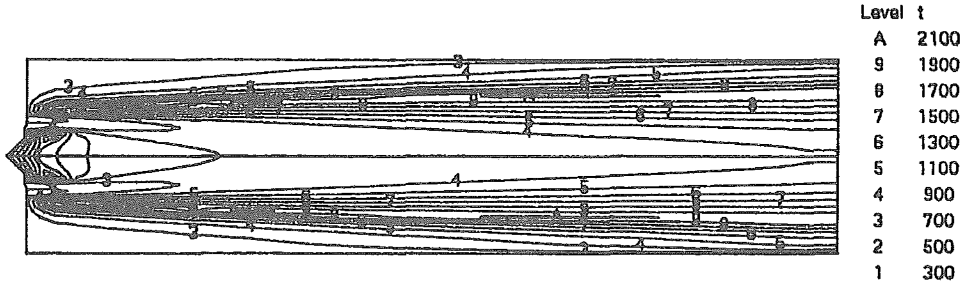

(b) a slit v-gutter

Fig. 4 The Predicted Temperature Distributions (Fast Chemistry)

bubble grows and the larger bubble weakens. Eventually the two bubbles merge to form a single recirculation zone. It is noted that if the slit flow does not follow the gutter wall, both the size and the strength of the bubble reduces. The above predictions are consistent with those observed experimentally in Ref. [9].

RESULTS AND DISCUSSIONS

Fig. 3 shows the the pictures of the flames in both of a conventional and a slit V-gutter. Fig. 4 demonstrates the predicted temperature distributions using the fast chemistry model. A similar prediction by the eddy-break-up model is also shown in Fig. 5.

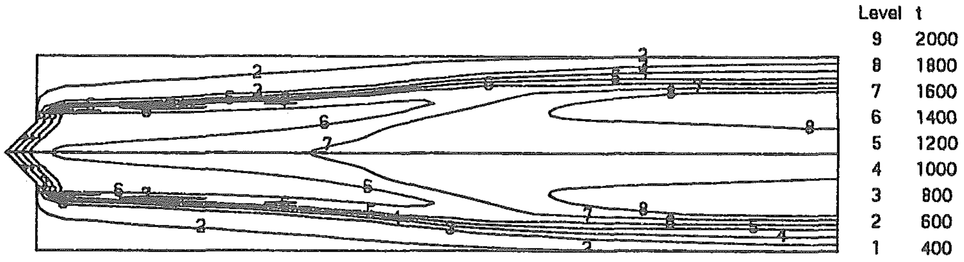

(a) a conventional v-gutter

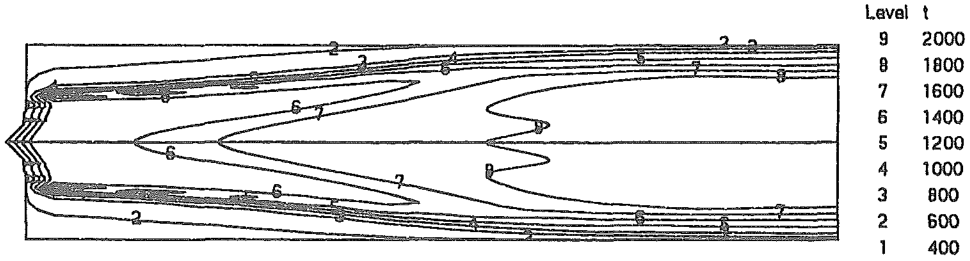

(b) a slit v-gutter

Fig. 5 The Predicted Temperature Distributions (EBU Model)

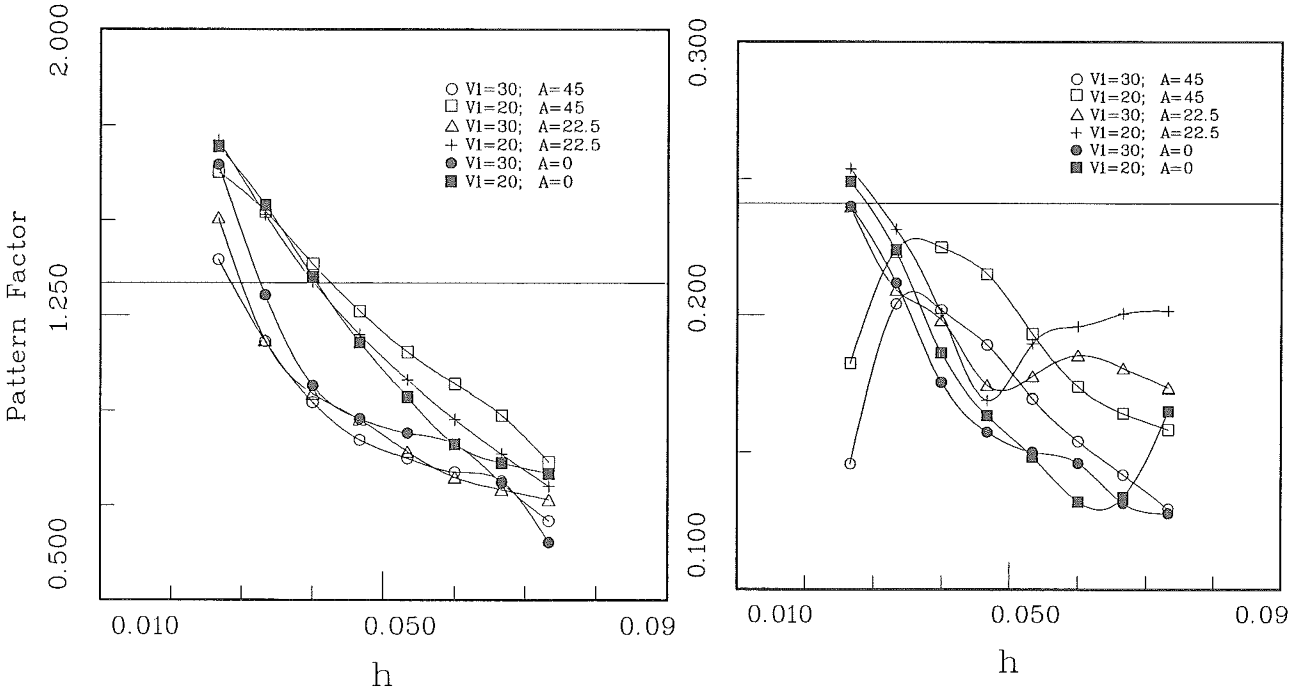

(a) fast chemistry model

(b) EBU model

Fig. 6 Pattern Factors as a Function of h.

Observing the temperature contours, it is found that the temperature is more evenly distributed in using the latter model. This is the characteristics of the eddy-break-up (EBU) model. In the fast chemistry model, the high temperature gradient is located in the shear layers anchored behind the gutter. Fig. 6 shows the pattern factors for the above two models. The values for the EBU model are significantly lower than those for the fast chemistry model. A higher pattern factor as h approaches the optimal value can be attributed to a more complete combustion. The effect of the slit height is studied. In Fig. 7, the length of the recirculation zone is shown to be a function of the slit height. As h increases the length as well as the strength of the recirculation zone (Fig. 8) decreases. Fig. 9 shows that the energy content in the recirculation zone decreases with h. As h increases to a certain value, there exists only a small bubble behind the inner ring of the gutter as shown in the previous study[15]. In this case, the flow field behind the outer ring actually departs from that behind the inner ring and can not provide an enhanced recirculation zone. Therefore, the v-gutter does not function properly. It is concluded that the slit height h should be carefully designed. In these figures, one also observes that the magnitude of the slit velocity and its angle have significant effects on the above parameters. In general, a higher slit velocity and an angle which follows the gutter wall can yield a stronger recirculation zone and a larger energy content. It seems that the slit "jet" between the two gutter walls extends the blocking area of the outer gutter and thus increases the effective blockage ratio. This shall favor a stable flame. The best arrangement studied is the configuration with V_1= 30 and A=45. There exists an optimum h which results in a maximal energy content. This is also true when EBU model is used as shown in Fig. 10.

It may be summarized that the performance of a slit v-gutter is strongly affected by the configuration of the slit. In addition to a larger slit velocity, a slit velocity angle which follows the gutter wall, the slit height has to be optimized for the best results.

From the results of the present study and the discussions in Ref. [9], it is believed that a slit V-gutter has the following advantages. First, the fuel-air ratio in the gutter can be adjusted by adding fuel through the slit flow. This can benefit the fuel-lean ignition as well as the lean blow-out limit. Second, the flame stabilization can be enhanced by adjusting the slit flow velocity as demonstrated in our calculation. Third, high

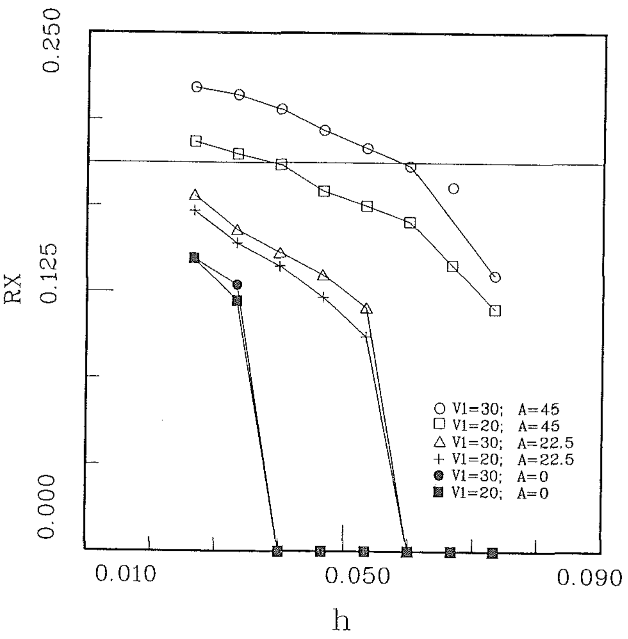

Fig. 7 Lengths of Recirculation Zone. (Fast Chemistry)

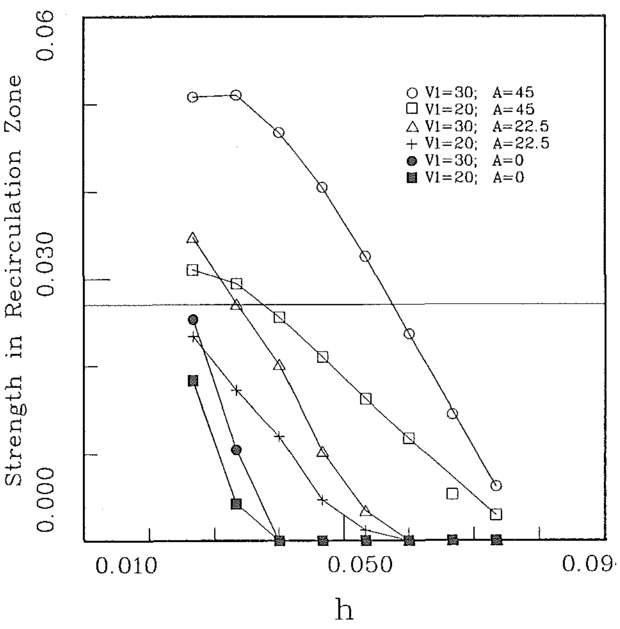

Fig. 8 Strength of Recirculation Zone. (Fast Chemistry)

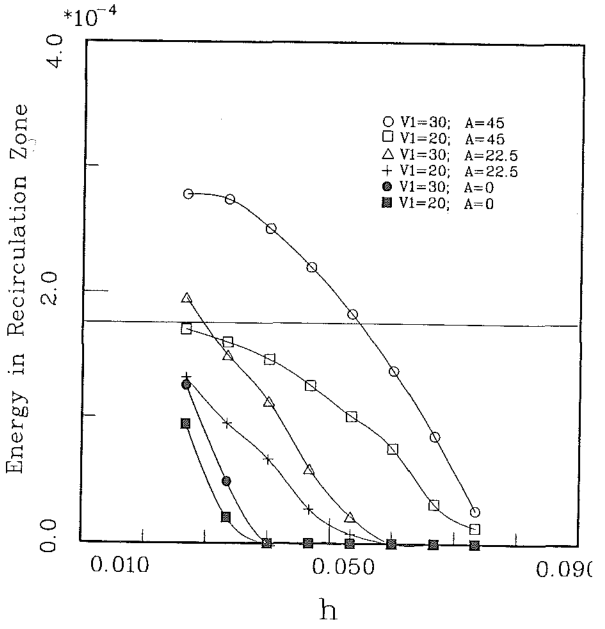

Fig. 9 Energy Content as a function of h. (Fast Chemistry)

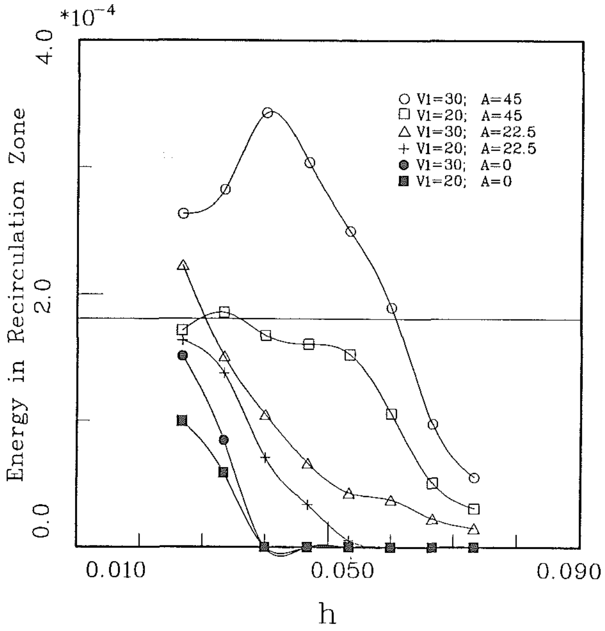

Fig.10 Energy Content as a function of h. (EBU Model)

temperature at the gutter wall can be partially controlled by utilizing a cool slit flow.

REFERENCES

1. E. W. Conrad, W. W. Velie and F. W. Schulze," A Study of Flameholder Elements for Use in High-velocity Afterburners," NACA RM E54J01, 1955.
2. B. T. Lundin, D. S. Gabriel and W. A. Fleming, " Summary of NACA Research on Afterburners for Turbojet Engines," NACA RM E55L12, 1956.
3. E. E. Zukoski and F. E. Marble," The Role of Wake Transition in the Process of Flame Stabilization on Bluff Bodies," in A. H. et al., (eds.) AGARD Combustion Researches and Reviews, Butterworths Publishing Co., London, pp.167-180, 1955.

4. B. Lewis and G. Von Elbe, Combustion, Flames and Explosions of Gases, pp. 436-446, Academic Press, New York, 1951.

5. J. M. Beer and N. A. Chigier, Combustion Aerodynamics, Chpt. 3, Robert Krieger Publishing Co., 1983.

6. A. H. Lefebvre, Gas Turbine Combustion, Chpt. 6, McGraw-Hill Book Co., 1983.

7. D. Lee, C. L. Yeh, Y. M. Tsuei, W. T. Jiang and Y. L. Chung," Numerical Simulation of Gas Turbine Combustor Flows, " AIAA Paper, 90-2305, 1990.

8. D. Lee and J. S. Lin, " Computation of Nonreacting Flows of a Two-Ring Flame Stabilizer Using A Zonal Grid Method," *Numerical Heat Transfer*, vol. 20, 65-79, 1991.

9. 王家驊,張許南'帶縫隙的 V形火焰穩定器,'國際航空第二期, pp. 39-40, 1988.

10. S. V. Patankar, " Numerical Heat Transfer and Fluid Flow," Hemisphere Publishing Co., New York, 1980.

11. D. Lee and J. J. Chiu, " A Covariant Velocity Based Calculation Procedure with Nonstaggered Grid for Computation of Pulsatile Flows," Numer. Heat Trans. 1992 (in press).

12. K. N. C. Bray, Turbulent Flows with Premixed Reactants, in Turbulent Reacting Flows, P. A. Libby and F. A. Williams (ed.), Springer-Verlag, New York, 1980.

13. L. S. Caretto and A. K. Runchal, Ramjet Combustor Modeling for Engine Design, AIAA Paper 89-2799, 1989.

14. D. Lee and Y. M. Tsuei, " LT-GRID, A Two-Dimensional Grid Generator," National Science Council Report CS75-0210-0006-04, Taiwan, 1987(in Chiness).

15. C. K. Lin, J. Chou, Y. M. Tsuei and D. Lee," A Numerical Study of Isothermal Flows of a Slit V-Gutter," AIAA Paper 92-0100, 1992.